

Grass and tree cover responses to intra-seasonal rainfall variability
vary along a rainfall gradient in African tropical grassy biomes

Original

Grass and tree cover responses to intra-seasonal rainfall variability
vary along a rainfall gradient in African tropical grassy biomes / D'Onofrio, D., Sweeney, L., von Hardenberg, J.,
Baudena, M.. - In: SCIENTIFIC REPORTS. - ISSN 2045-2322. - 9:(2019). [10.1038/s41598-019-38933-9]

Availability:

This version is available at: 11583/2814868 since: 2020-04-22T12:55:16Z

Publisher:

NATURE PUBLISHING GROUP

Published

DOI:10.1038/s41598-019-38933-9

Terms of use:

This article is made available under terms and conditions as specified in the corresponding bibliographic description in
the repository

Publisher copyright

(Article begins on next page)

SCIENTIFIC REPORTS



OPEN

Grass and tree cover responses to intra-seasonal rainfall variability vary along a rainfall gradient in African tropical grassy biomes

Donatella D'Onofrio^{1,2}, Luke Sweeney², Jost von Hardenberg¹ & Mara Baudena²

Although it is well known that mean annual rainfall (MAR) and rainfall seasonality have a key role in influencing the distribution of tree and grass cover in African tropical grassy biomes (TGBs), the impact of intra-seasonal rainfall variability on these distributions is less agreed upon. Since the prevalent mechanisms determining biome occurrence and distribution change with MAR, this research investigates the role of intra-seasonal rainfall variability for three different MAR ranges, assessing satellite data on grass and tree cover, rainfall and fire intervals at a sub-continental scale in sub-Saharan Africa. For MAR below 630 mm y⁻¹, rainfall frequency had a positive relationship with grass cover; this relationship however became mostly negative at intermediate MAR (630–1200 mm y⁻¹), where tree cover correspondingly mostly increased with rainfall frequency. In humid TGBs, tree cover decreased with rainfall intensity. Overall, intra-seasonal rainfall variability plays a role in determining vegetation cover, especially in mesic TGBs, where the relative dominance of trees and grasses has previously been largely unexplained. Importantly, the direction of the effect of intra-seasonal variability changes with MAR. Given the predicted increases in rainfall intensity in Africa as a consequence of climate change, the effects on TGBs are thus likely to vary depending on the MAR levels.

Grasslands and savannas, known together as tropical grassy biomes (TGBs), are estimated to cover ca. a third of Africa and a fifth of the world's land area^{1,2}. Characterised by continuous C₄ grassland, and possible coexistence with trees², they support a growing proportion of the world's population, are home to the majority of the world's remaining megafauna² and are a critical store of biodiversity³. Despite their importance, TGBs have garnered little public attention or conservation effort in comparison to tropical forests^{1,4}, and the role of grass in characterizing these biomes has only recently been studied at sub-continental level⁵.

The relative dominance of trees and grasses in TGBs and the extent of those systems are governed by numerous feedbacks between bottom-up factors (*sensu* ref.⁴), such as water availability and soil type, and by top-down factors, such as fire and herbivory (ref.⁶ and references therein). Mean annual rainfall (MAR) has been identified as the most important factor, both impacting the availability of water and seemingly influencing the relative importance of other factors^{5,7–9}. Whereas tree and grass cover is limited primarily by water availability in dry TGBs, in mesic areas the high fire frequency, fostered by high grass cover, helps to limit tree cover^{5,7}. At these higher MAR levels, both tropical forests and savannas exist^{10–12}, with savannas mostly observed in areas with highly seasonal rainfall regimes, but partly also under overlapping climatic conditions with forests^{5,11,13}. In these areas TGBs are probably maintained by a grass-fire feedback, whereby grasses provide fuel for fire, which in turn restricts the recruitment and growth of shade-tolerant and fire-intolerant forest trees, thus supporting the growth of grasses and fire-resistant savanna trees¹⁴. Generally, for mesic savannas, the ability to predict the relative dominance of tree and grass cover remains limited⁵.

In TGBs, competition for water by trees and grasses leads to water resource partitioning by root depth¹⁵, with root-depth separation between trees and grasses observed in dry areas^{16,17}. Variations in rooting depth by

¹Institute of Atmospheric Sciences and Climate, National Research Council (ISAC-CNR), Corso Fiume 4, 10133, Torino, Italy. ²Copernicus Institute of Sustainable Development, Environmental Science Group, Utrecht University, Princetonlaan 8a, 3584 CB, Utrecht, The Netherlands. Donatella D'Onofrio and Luke Sweeney contributed equally. Correspondence and requests for materials should be addressed to D.D. (email: d.donofrio@isac.cnr.it) or L.S. (email: lukesweeney264@gmail.com) or M.B. (email: m.baudena@uu.nl)

vegetation type have been demonstrated in TGBs across differing rainfall gradients, with tree roots becoming shallower with MAR and overlapping with grass roots at higher rainfall levels¹⁸.

Soil water content depends not only on yearly rainfall levels or on rainfall seasonality, but also on the temporal distribution of rainfall within a season, described here as rainfall event frequency and intensity¹⁹. The intra-seasonal temporal distribution of rainfall can influence vegetation productivity dramatically^{20,21}, especially in dry areas^{22–24}, and it can affect the outcome of competition between plants with different water strategies^{25–27}. Mirroring changes observed in global precipitation variability²⁸, changes in rainfall patterns have been observed across Africa over several decades in the last century, with, for example, increases in rainfall intensity in Southern and Western Africa^{29,30}, reductions in rainfall frequency specifically in Botswana³¹, decreases in intensity in Central Africa³², and increases in drought length across Eastern Africa³³. Changes in rainfall variability have been closely associated with anthropogenic climate change³⁴, and, with rainfall intensity in Africa expected to increase in the future³⁵, changes in vegetation patterns may result.

Although a substantial body of research now exists in relation to TGBs and the role of various factors in explaining their occurrence and extent, the relative importance of intra-seasonal rainfall variability is less clearly understood. Recent research on the impact of intra-annual variability of rainfall on tree cover for different MAR ranges in Africa⁹ and across tropical areas³⁶ has shown that intra-annual variability has an important role in determining tree cover variation, particularly within the intermediate (500–1500 mm y⁻¹) MAR levels³⁶. However, the influence of intra-seasonal variability on tree cover depends upon MAR throughout tropical Africa^{36,37}, specifically for TGBs⁹. In drier TGBs, tree cover can increase with rainfall intensity⁹, in line with experimental work³⁸ showing that increased precipitation intensity increases deep soil water, enhancing woody plant growth; this is supported by the deeper roots observed for trees than for grasses in drier savannas^{17,18,39}. These findings are corroborated by modelling work²⁵ that includes competition of grasses with tree seedlings, suggesting that more rare and intense rainfall events support the growth of woody plants in arid savannas, due to the out-competition of grasses on tree seedling, an effect which is especially strong at low moisture availability^{40,41}. In contrast, areas with lower tree cover in African TGBs have been associated with greater rainfall intensity (although the precise impact depends also on soil type)⁹ which is analogous to that reported by ref.⁴² with data across all African biomes. This finding has been modelled and explained by the different relative-growth rates of grasses and trees⁴³ (*sensu* ref.⁴⁴), with grasses having the ability to grow faster than trees in the presence of high soil moisture, but being more negatively impacted under high water stress.

Within this context, the main research question addressed in this paper is whether changes in intra-seasonal rainfall variability affect the propensity of grasses, in addition to trees, to grow in TGBs at different MAR ranges. Given the importance of grasses in determining TGB extent and existence¹ and their important role in the competition for water with trees², we explicitly included grass cover as a dependent variable, unlike previous, similar studies that analysed large scale satellite data and considered only the tree cover variable^{9,36,42}. In so doing we consider the interaction between vegetation types in TGBs at a sub-continental scale. Following a methodological approach closely aligned to that of ref.⁵, which analysed grass cover for the first time at sub-continental scale, we analysed the impact of intra-seasonal temporal variability of rainfall on grass and tree cover at sub-continental scale throughout TGBs in sub-Saharan Africa, in comparison to the impact of fire, MAR and rainfall seasonality (analysed in ref.⁵). As in that earlier study, we assessed separately three different MAR ranges, since different explanatory variables are relevant for low (less than 630 mm y⁻¹), intermediate (between 630 mm y⁻¹ and 1200 mm y⁻¹), and high MAR (above 1200 mm y⁻¹). The analysis by MAR range enhances the ability to identify the factors, in addition to rainfall totals, that can explain differences in tree and grass cover, potentially identifying a role for intra-seasonal variability that may have otherwise been overlooked.

Material and Methods

Satellite data. We analysed gridded data at 0.5° resolution of observed percentages of tree (T) and grass (G) cover in areas of tropical grassy biomes in sub-Saharan Africa (between 35°S and 15°N) as a function of four different rainfall variables and average fire interval data (AFI, [y]). The rainfall variables were mean annual rainfall (MAR, [mm y⁻¹]), average rainfall seasonality index (SI) and two variables representing intra-seasonal rainfall variability: average wet-season daily rainfall frequency (λ_w , [d⁻¹]) and intensity (α_w , [mm d⁻¹]). All variables were averaged over the period 2000–2010. Vegetation cover, fire intervals, mean annual rainfall and rainfall seasonality were calculated following ref.⁵, and as detailed below.

We used the daily rainfall measurements of the tropical rainfall measuring mission (TRMM 3B42), with 0.25° original resolution, to derive MAR, SI⁴⁵, α_w and λ_w ²⁴. As in ref.⁵ we considered grid cells with MAR up to 2500 mm y⁻¹. SI is defined by Walsh & Lawler as a ratio with the absolute value of the sum of the differences between monthly rainfall and average monthly rainfall at the numerator and annual rainfall at the denominator. It can range from 0 (if the annual rainfall is equally distributed over the year) to 1.83 (if all the annual rainfall falls in one month). In seasonal environments, such as those associated with savannas, precipitation affects plants mainly during the growing period^{46,47}. For this reason, the estimation of daily rainfall intensity and frequency over the wet seasons is more appropriate than over the year. We thus assumed that the wet seasons correspond to the growing seasons of both plant types (although this may not be strictly true for all savannas, see refs^{2,48} and references therein). For each grid cell, α_w was computed as the mean, over the years, of the daily rainfall in the wet days (assumed as days with precipitation greater than 0.1 mm d⁻¹) within the wet periods (identified as explained in the following paragraph). The small threshold was introduced to take into account observation measurement errors. For each grid cell, λ_w was calculated as the ratio of the average number of wet days to the average length of the wet periods (L_w , [d], calculated as explained in the following paragraph). α_w and λ_w were defined such that the following relation was verified: $MAR_w = \alpha_w \cdot \lambda_w \cdot L_w + c$, where MAR_w is the wet-season mean annual rainfall and c is the sum of the

rainfall occurring in the wet-season days in which rainfall is smaller than 0.1 mm d^{-1} ; across the data analysed, c was 0.30 mm y^{-1} on average. Consequently, MAR_w , L_w , α_w and λ_w are not independent of each other.

To calculate the wet-season length L_w , we identified the wet periods as the months in which mean precipitation was greater than a percent threshold p_{thr} of the climatological annual average monthly rainfall. Then, by summing up the lengths in days of these wet months and dividing by the number of years, we obtained the average wet season length L_w . To decide upon the threshold p_{thr} , we maximised the correlation of L_w with the length of the wet season calculated with an alternative method, which was related to the opposite of SI ($L_{w,\text{SI}}$), similarly to that used by ref.⁴², i.e.: $L_{w,\text{SI}} = 365/12 [11 \cdot (1 - \text{SI}/1.83) + 1]$, so that $L_{w,\text{SI}}$ is equal to ca. 30 d for $\text{SI}_{\text{max}} = 1.83$ and to 365 d for $\text{SI}_{\text{min}} = 0$ ⁴⁵. We chose $p_{\text{thr}} = 50\%$, as for this value the two measures of wet season length were highly correlated ($R^2 = 0.96$).

We obtained the annual average fire interval (AFI) from the monthly MCD45A1 burnt area satellite product (Collection 5.1), with original 500 m resolution, available from April 2000^{49–51}. AFI is the expected return time of fire at any point in the 0.5° grid cell⁵², calculated as the inverse of the average annual burnt area fraction (BA, [y^{-1}]) in each 0.5° grid cell ($\text{AFI} = 1/\text{BA}$). BA was obtained following the method used by ref.⁵³. In the analysis we used $\log_{10}(\text{AFI})$ (equal to $-\log_{10}(\text{BA})$), because AFI covered several orders of magnitude. In order to avoid infinity values of AFI (when $\text{BA} = 0$), we set the maximum of AFI to 10,000 years adding to BA a small constant (0.0001 y^{-1}) (see also ref.⁵).

Percentages of tree cover (T) and grass cover (G) were obtained from the annual tree and non-tree vegetation cover products, respectively, of the Terra MODIS Vegetation Continuous Fields product (MOD44B, V051), with original 250 m resolution⁵⁴. Since MODIS tends to underestimate tree cover in the presence of shrub⁵⁵, we used the 300-m ESA global land cover map (ESA CCI-LC, v 1.6.1; 5-year-averaged dataset centred in 2010) to remove grid cells with more than 50% of the area covered by shrublands (ESA CCI-LC codes 120,122). We used the same land cover map to mask out grid cells with more than 33% of the area influenced by humans, such as cropland/urban areas, and/or covered by water (codes $\leq 40, 190, 210$) and/or covered by permanent snow or ice (code 220). This conservative choice, motivated by the inclusion of areas with only minimal human impact, selected a representative range of areas in sub-Saharan Africa. See also ref.⁵ for more details.

In order to study the effect of the abiotic variables specifically on tropical grassy biome vegetation, we identified grid cells of TGBs as those with more than 50% of the area flagged on the ESA CCI-LC map as deciduous trees and grassland (codes 60–62,130), following ref.⁵. This choice was based on the fact that African savannas trees are mostly deciduous (refs^{56,57}, and see literature review in ref.⁵). The use of this method for distinguishing TGBs avoided problems in identifying biomes based on tree cover discontinuities in MODIS data⁵⁸. The final datasets consisted of 1692 grid cells.

Statistical modelling. We analysed the relationships between vegetation cover variables (T and G) and five abiotic variables (MAR , SI, λ_w , α_w and $\log_{10}(\text{AFI})$) using generalized linear models (GLM)⁵⁹, in three different MAR ranges: $0\text{--}630 \text{ mm y}^{-1}$ (R1), $630\text{--}1200 \text{ mm y}^{-1}$ (R2) and $1200\text{--}2500 \text{ mm y}^{-1}$ (R3). These have been determined in the study of ref.⁵ and highlight how MAR influences the role of the prevalent mechanisms related to water availability and fire in determining biome occurrence and tree to grass dominance in sub-Saharan Africa. See a map of their spatial distribution in Supplementary Fig. S1. Figure 1 shows the variable distributions in these three ranges. For completeness, we also repeated the GLM analysis for all the TGB data, without filtering by MAR ranges. Notice that we did not include MAR_w and L_w in the statistical analysis because MAR_w was highly correlated with MAR ($R^2 > 0.98$ for each of the three ranges), and L_w was anti-correlated with SI ($R^2 > 0.94$ for each of the three ranges). In R1, R2 and R3 there were 694, 783 and 215 grid cells, respectively. We tested that the medians of the variable distributions were statistically different at the 5% significance level using the two-sided Wilcoxon rank sum test.

Tree and grass cover fractions were fitted assuming a binomial error distribution with a logit link function, because they are bounded between 0 and 1^{60,61}. We investigated the relationships considering models with different terms of a single predictor up to the third order, and models with a combination of the predictors but including only linear terms. Predictor variables were standardized subtracting their mean and dividing their standard deviation, such that their coefficient magnitude was a measure of their importance in the model. Since the rainfall variables used were not independent of each other (see previous section), we decided to exclude models containing both α_w and λ_w . We included also the intercept-only model (i.e., a constant model), obtaining a set of 34 possible models. Models were selected based on the Akaike's information criterion (AIC)⁶², such that the best models were those with the lowest AIC value, and we reported the ΔAIC (i.e. the difference between the AIC value of each model with the best model). We analysed all models with AIC smaller than the model including the intercept-only. The goodness-of-fit was evaluated as the fraction of least-squares explained (pseudo- R^2 , R^2 in the following for brevity), equivalent to the explained variance in a linear least-squares regression model⁶³. It was computed as $R^2 = 1 - D_m/D_0$, where D_m is the residual deviance, i.e. the deviance that remains unexplained by the fit, and D_0 is the deviance of the intercept-only model^{61,63}.

To take into account collinearity between explanatory variables (see Supplementary Table S1 for the Pearson's r value of the variables in each of the three ranges), we performed a residual analysis for the cases where the best model included α_w or λ_w . This analysis was aimed at understanding whether the influence of these predictors on the vegetation cover was independent of the other explanatory variables. To this end, we computed the GLM of each intra-seasonal rainfall variable (α_w or λ_w) as a function of MAR, SI and $\log_{10}(\text{AFI})$ (see also Supplementary Note S1 for details), and computed the deviance residuals. We calculated also the deviance residuals of the vegetation cover GLM computed with respect to the same three explanatory variables (as obtained from the above-described analyses). We then calculated the R^2 of the linear fit of these two residual sets, as a high R^2 implied that the dependence of the vegetation cover variable on α_w or λ_w was direct and not only mediated by the other variables.

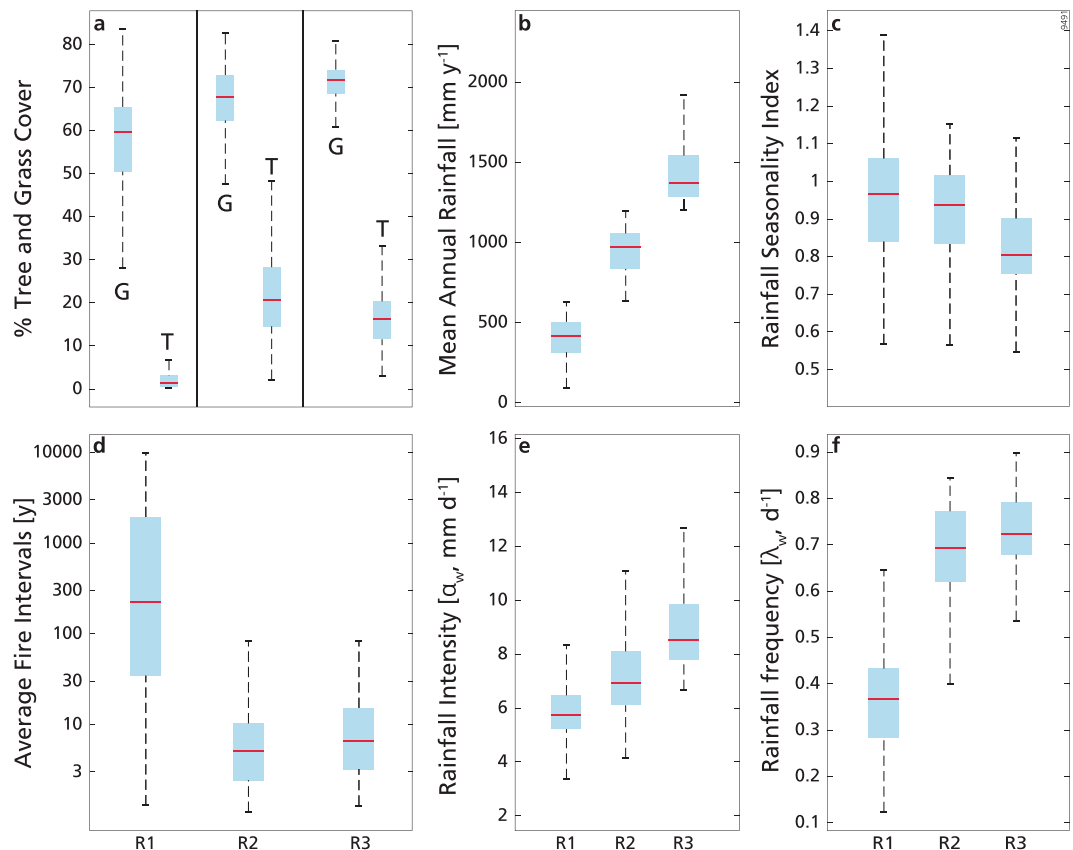


Figure 1. Box plots of percentage cover of tree (T) and grass (G) (a), mean annual rainfall (b), rainfall seasonality index (c), average fire intervals (d), wet-season daily rainfall intensity (e) and wet-season daily rainfall frequency (f), in the low (R1; $\text{MAR} \leq 630 \text{ mm y}^{-1}$), intermediate (R2; $630 \text{ mm y}^{-1} < \text{MAR} < 1200 \text{ mm y}^{-1}$) and high (R3; $\text{MAR} \geq 1200 \text{ mm y}^{-1}$) MAR ranges. Outliers are not shown. All the distribution medians differed significantly.

MAR range	Vegetation cover	Best model	R ²
R1-Low MAR	Tree	$\text{logit}(T) = -3.85 + 0.55 \cdot \text{MAR}$	0.22
	Grass	$\text{logit}(G) = 0.22 - 0.42 \cdot \text{SI} + 0.38 \cdot \lambda_w$	0.56
R2-Intermediate MAR	Tree	$\text{logit}(T) = -1.48 + 0.49 \cdot \lambda_w + 0.14 \cdot \lambda_w^2$	0.38
	Grass	$\text{logit}(G) = 0.73 - 0.17 \cdot \log_{10}(\text{AFI}) - 0.17 \cdot \lambda_w$	0.37
R3-High MAR	Tree	$\text{logit}(T) = -1.62 - 0.41 \cdot \alpha_w$	0.32

Table 1. Best GLMs for tree cover (T) and grass cover (G) in the three mean annual rainfall (MAR) ranges: low MAR (R1, $\text{MAR} \leq 630 \text{ mm y}^{-1}$), intermediate MAR (R2, $630 \text{ mm y}^{-1} < \text{MAR} < 1200 \text{ mm y}^{-1}$) and high MAR (R3, $\text{MAR} \geq 1200 \text{ mm y}^{-1}$). Predictors are: MAR, rainfall seasonality index (SI), logarithmic average fire interval ($\log_{10}(\text{AFI})$), wet-season daily rainfall intensity (α_w) and wet-season daily rainfall frequency λ_w . Predictor variables were standardized such that in the GLMs their coefficient magnitude is a measure of their importance in the model. Best models were those with the smaller Akaike information criterion (AIC), see Supplementary Tables S2–S6. No significant model was found for grass cover in R3. The explained deviance (R²) is reported for each case. See Material and Methods in the main text for a detailed description of the statistical models and selection procedures.

Data analysis was performed using MATLAB R2015b. In particular, we used the Matlab function ‘fitglm’, for the GLM analysis, and ‘ranksum’ for the Wilcoxon rank sum test.

Results

In each MAR range, one of the intra-season rainfall variables (α_w or λ_w) always appeared in the best model for either T or G (or both). Yet, when performing the analysis without distinguishing between MAR ranges (i.e. analysing all the dataset at once), the intra-seasonal rainfall variables did not appear in any of the best models: according to these models T depended on MAR and G on both SI and $\log_{10}(\text{AFI})$ (see Supplementary Tables S7 and S8). In the following, we report the results of the statistical analysis computed in each MAR range separately.

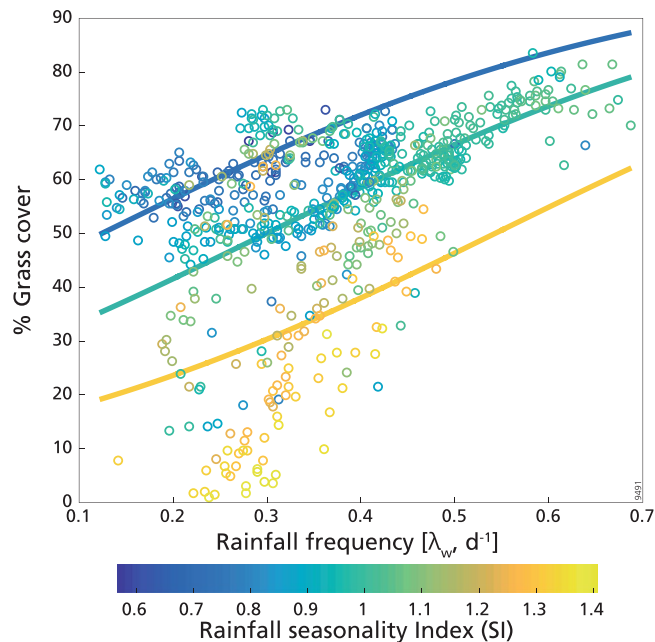


Figure 2. Percentage cover of grass in low mean annual rainfall range ($\text{MAR} \leq 630 \text{ mm y}^{-1}$) as a function of wet-season rainfall frequency (λ_w). Colours indicate the seasonality index (SI): for increasing values of SI rainfall occurs in less months during the year. Continuous lines are the best model fit for grass (see Table 1) computed with the median value of SI (equal to 0.97, central line), the 95th percentile (equal to 1.3, lower line) and the 5th percentile (equal to 0.72, higher line).

$\text{MAR} \leq 630 \text{ mm y}^{-1}$. For low precipitation areas, T was mainly determined by MAR, while λ_w and SI were both included in the best model for G (Table 1).

Specifically, T had a positive trend with MAR ($R^2 = 0.22$), which is the most important factor among those we considered in explaining tree cover variations in this range. The inclusion of other rainfall variables in models with MAR only increased the explained deviance by a small amount (ca. 0.04–0.05) (Supplementary Table S2). Tree cover decreased with λ_w and SI, and increased with α_w , however, all of the selected models had an AIC close to the intercept-only model, indicating that they were weak.

According to the best model, G, which ranges from ca. 30% to ca. 80% (Fig. 1a), decreased with SI, i.e. it was larger where precipitation was less seasonal, and increased with λ_w , that is, it was larger where rainfall events were more frequent (Fig. 2). The magnitude of the predictor's standardized coefficients was similar, and this model could explain 56% of the deviance (see Table 1 and Supplementary Table S3). Although λ_w was present in the best model, its effective role on G variations should be analysed in the light of its collinearity with other predictors, and in particular with MAR ($r = 0.73$, Supplementary Table S1). This was evident from the analyses of the following models and of the residuals. The best models with SI and MAR alone (cubic logit fit, $\Delta\text{AIC} = 4.10$, and linear logit fit, $\Delta\text{AIC} = 10.86$, respectively, Supplementary Table S3) could explain a much larger fraction of the deviance (53% and 40%, respectively) than the best model with λ_w alone (parabolic logit fit, $\Delta\text{AIC} = 26.28$, $R^2 = 0.23$; in the following we will use 'parabolic fit' to indicate 'parabolic logit fit'). The other explanatory variables ($\log_{10}(\text{AFI})$ and α_w) had smaller importance (Supplementary Table S3).

From the residual analysis (see Supplementary Note S1) we found that the linear relationship between the residuals of λ_w and G was associated with a small correlation coefficient ($R^2 = 0.07$). This indicated that the precipitation frequency variable did not have an important role in determining G without the influence of the other predictors. In fact, λ_w , as expected, was highly determined by MAR, SI and $\log_{10}(\text{AFI})$ (in order of importance), which together explained 69% of the deviance for λ_w (Supplementary Table S9). Therefore, the increase of G with λ_w could be interpreted as due to the simultaneous changes of the other factors: in particular, λ_w , and consequently G, was higher in areas with higher MAR (which had the largest coefficient in the model).

$630 \text{ mm y}^{-1} < \text{MAR} < 1200 \text{ mm y}^{-1}$. For intermediate precipitation, the best model for T included only λ_w , through a parabolic fit that explained 38% of the deviance (Fig. 3a, Table 1), while G was mostly explained by $\log_{10}(\text{AFI})$ and λ_w together ($R^2 = 0.37$, Table 1, Fig. 3b), showing an opposite dependence on λ_w with respect to the low rainfall range. The decreasing trend of grass cover with $\log_{10}(\text{AFI})$ in this range confirmed the findings of ref.⁵, whose results are comparable in this range as the vast majority of the areas with such MAR in sub-Saharan Africa are covered by TGBs.

According to the best model shown in Fig. 3a, T, which in this range had the larger variation with respect to the other two MAR ranges (Fig. 1a), increased with daily rainfall frequency from 0.45 d^{-1} (obtained from the minimum of the parabolic fit) to ca. 0.85 d^{-1} , but varied less for λ_w below 0.45 d^{-1} (Fig. 3a). λ_w was present in the first 10 models ($\Delta\text{AIC} < 3$), in which it always had greater importance than the other variables (Supplementary

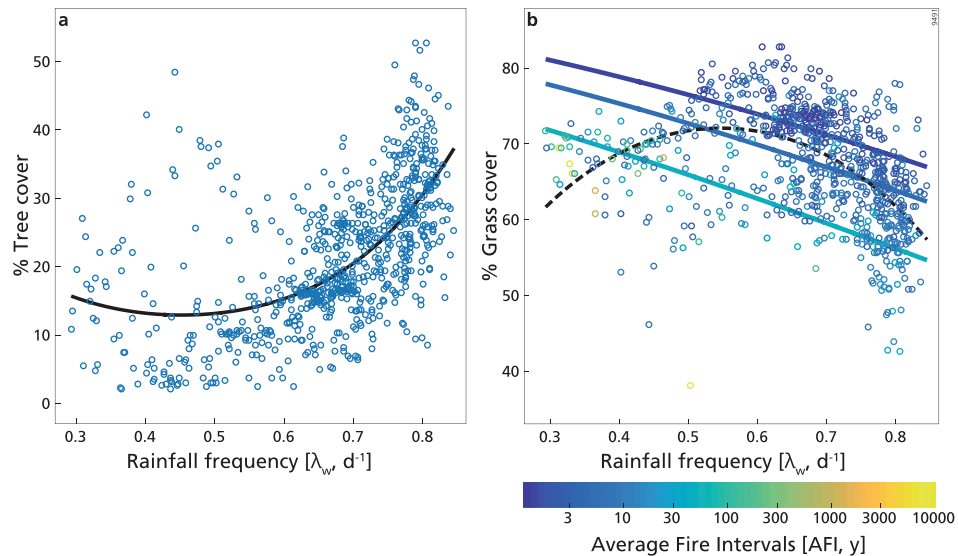


Figure 3. Percentage cover of tree (a) and grass (b) in the intermediate mean annual rainfall range ($630 \text{ mm y}^{-1} < \text{MAR} < 1200 \text{ mm y}^{-1}$) as a function of wet-season rainfall frequency (λ_w). (a) Continuous line is the best model fit (see Table 1). (b) Continuous lines are the best model fit for grass cover (see Table 1) computed with the median value of AFI (equal to 5 y, central line), the 95th percentile (equal to 47 y, lower line) and the 5th percentile (equal to 1.3 y, higher line). Colours indicate the average fire intervals (AFI). Dashed line indicates the fit of the best model between grass cover and λ_w (Supplementary Table S5).

Table S4). Looking at the contribution of the other factors, T generally increased with MAR, $\log_{10}(\text{AFI})$, SI and decreased with α_w (Supplementary Table S4). However, the dependence of T on these variables alone was very weak (i.e. they had an AIC close to the intercept-only model), and generally explained low deviance ($R^2 \leq 0.17$; Supplementary Table S4), in line with findings from ref.⁵ (though for MAR, $\log_{10}(\text{AFI})$ and SI only).

According to the best model, G decreased with rainfall frequency, and (similarly to ref.⁵) decreased with the average fire intervals ($\log_{10}(\text{AFI})$), i.e. it was favoured by increasing fire frequency (Fig. 3b, Table 1). The model with λ_w alone (parabolic fit, third selected model with $\Delta\text{AIC} = 1.72$, $R^2 = 0.27$, Supplementary Table S5) indicated that G was disadvantaged by increasing precipitation frequency only for λ_w greater than 0.55 d^{-1} (obtained from the maximum of the parabolic fit, Fig. 3b), whereas the opposite occurred for lower λ_w (Fig. 3b). Interestingly, the maximum of the parabolic fit between G and λ_w was relatively close to the minimum of the parabolic fit of T with λ_w . However, the dependence of G on λ_w alone was quite weak (AIC close to the intercept-only model), and this was the case also for the other selected models. SI and MAR were present in models with AIC smaller than the intercept-only model but gave negligible contributions to the explained deviance (Supplementary Table S5).

Through the residual analysis (Supplementary Note S1), we verified that the tendencies of both T and G to increase or decrease in the two parts of their parabolic fits with λ_w were independent from MAR, SI and $\log_{10}(\text{AFI})$, as expected also from the smaller correlation coefficients between predictors in R2 (Supplementary Table S1). Thus, the positive dependence of T on λ_w (for $\lambda_w > 0.45 \text{ d}^{-1}$) and the negative one of G (for $\lambda_w > 0.55 \text{ d}^{-1}$) were valid for every value of the other explanatory variables and the correlations with the residuals of λ_w of the residuals of T was $R^2 = 0.36$ and of the residuals of G was $R^2 = 0.31$ (Supplementary Fig. S2).

MAR $\geq 1200 \text{ mm y}^{-1}$. At high precipitation, we found that T mainly depended on α_w (Fig. 4), while G was not explained by any explanatory variable (Table 1).

α_w was the factor determining most of the variation of T, with decreases in the variable associated with increasing rainfall intensity (Fig. 4, Table 1). This dependence could explain 32% of the deviance for T. There was also a tendency of T to decrease with $\log_{10}(\text{AFI})$, but this dependence was very weak (Supplementary Table S6). Models with MAR, SI and λ_w had AIC greater than the intercept-only model, thus they didn't play any role.

After removing the influence of MAR, SI and $\log_{10}(\text{AFI})$ from both T and α_w , we found that the decreasing of T with α_w was preserved, although the importance of this dependence decreased ($R^2 = 0.20$, see Supplementary Fig. S2). In fact, the variation of α_w was highly determined by SI, MAR and $\log_{10}(\text{AFI})$ (in order of importance, $R^2 = 0.66$, Supplementary Table S9), as expected also from the correlation coefficients between predictors (Supplementary Table S1). Therefore, T decreased with α_w partially as a consequence of the simultaneously increase of the latter with MAR, SI and $\log_{10}(\text{AFI})$. In other words, T was smaller in areas with higher α_w partly because they corresponded to areas of higher MAR, higher rainfall seasonality and rare fires.

Discussion

Our results appear to indicate that intra-seasonal rainfall variability has a role to play in determining the relative predominance of grasses and trees in TGBs in sub-Saharan Africa, with that role and importance dependent on mean annual rainfall (MAR) levels. At the low and intermediate rainfall ranges, the frequency of rainfall during the rainy season was included in the best models explaining grass cover, yet with opposite effects: grasses show a

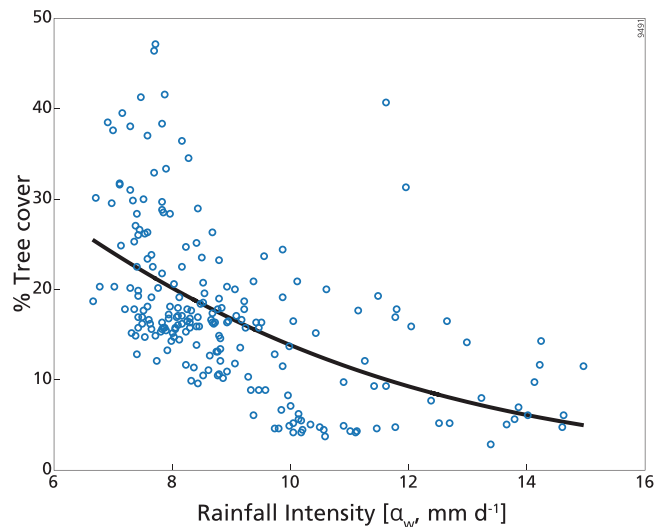


Figure 4. Percentage cover of tree in the high mean annual rainfall range ($\text{MAR} \geq 1200 \text{ mm y}^{-1}$) as a function of wet-season rainfall intensity (α_w). Continuous line is the best model fit (see Table 1).

positive (although noisy) trend with rainfall frequency at the dry end of the gradient, while they show a negative trend with it in mesic TGBs, which is especially evident for the highest rainfall frequencies. At this intermediate rainfall level, tree cover also increased with average rainfall frequency in the wet season for the most part, and, somewhat analogously, in the humid TGBs tree cover decreased with rainfall intensity. Importantly, average rainfall frequency in the wet season was shown to explain a reasonable share of the deviance at the intermediate rainfall level for grasses and trees for the first time. The relative importance of intra-seasonal rainfall variability is somewhat lost when investigating the vegetation responses for all TGBs across the sub-continent, with MAR the dominant factor for trees, and seasonality and average fire interval most important for grasses. This highlights the importance of disaggregating the results by MAR range, as the main mechanisms governing TGB dynamics vary with absolute rainfall values^{5,7,9}. Differing responses of grass and tree cover to intra-seasonal rainfall variability at different rainfall levels seem to explain the contrasting findings in relation to intra-seasonal variability highlighted by previous research^{38,42}.

For grasses, the positive relationship between rainfall frequency and grass cover at the lower MAR level is similar to earlier modelling results for dry savannas²⁵. Given that increases in rainfall frequency can enhance water availability in surface soils^{19,64}, our finding is consistent with observations regarding the ability of grasses to extract shallow soil water in comparison to trees^{65–67}. At lower rainfall levels, the difference between grass root depth and tree root depth is large^{18,68}, suggesting a more shallow soil moisture profile would favour grasses, as they also have a more aggressive uptake strategy with respect to trees in dry savannas^{16,69}. This result is in line with earlier experimental work³⁸, based on a study site with MAR of 544 mm y^{-1} , where it was found that increases in intensity and, by virtue of the experimental design, reduction in rainfall frequency, push soil moisture deeper into the soil, benefitting trees with deeper roots at the expense of shallow rooted grasses. In line with this, we also observed, as in other studies^{9,36}, that in dry TGBs trees, which are deeper rooted than grasses at this MAR range, increased in cover with more intense, less frequent rainfall. Trees have also access to deeper water during the dryer periods of the year⁶⁶, and increased rainfall intensity with reduced rainfall frequency would assist in enhancing the competitive advantage of trees by increasing deep water recharge. However, it must be noted that intra-seasonal rainfall variables explained a very small part of the deviance for tree cover, which mainly depended on MAR, possibly indicating that tree growth is generally water-limited in these areas. Furthermore, our residual analysis showed that part of the deviance for grass cover explained by rainfall frequency at the lower MAR range is in fact due to its collinearity with the other independent variables, especially with rainfall seasonality and annual amounts. Rainfall seasonality plays a large role at the low MAR range, explaining a large share of the variation for grass cover on its own ($R^2 = 0.53$). This implies that of the two variables included in the best model for grasses, seasonality is by far more important than rainfall frequency. It is also important to note that rainfall frequency is also closely correlated with MAR (Pearson's $r = 0.73$), and a model including MAR alone explains 40% of the deviance for the grass cover; this highlights the importance, in this low range, of the absolute levels of the water resource for both grasses and trees, as already observed for dry sub-Saharan biomes in general⁵. This may also help to explain why it is rainfall frequency, as opposed to rainfall intensity, that is included in the best model for grass cover, as rainfall intensity shows a much lower correlation with MAR in this range (Pearson's $r = 0.14$).

In contrast to the findings for grass cover in the low MAR range, in the intermediate rainfall range, increases in rainfall frequency in the rainy season were associated with a reduction in grass cover for average rainfall frequencies above 0.55 d^{-1} . Contrasting responses along a rainfall gradient have been observed previously for grasses in North American prairies⁷⁰, and recently for trees in African TGBs⁹ and across the global tropics³⁶. This tendency of grassland to prefer less frequent rainfall at this range is similar to that observed in few experimental field sites in Africa⁷¹ as well as in other parts of the globe (e.g. ref.⁷²). In this intermediate rainfall range, we also observe a

positive relationship between tree cover and rainfall frequency (above 0.45 d^{-1}), confirming previous results^{9,36,42}. While TGB grass cover has been largely unexplained so far in this intermediate range (Supplementary Table S5), more than a quarter of the deviance for grass cover is explained by rainfall frequency alone ($R^2 = 0.27$). As previously mentioned, in these mesic savannas there is greater overlap between tree and grass root depth compared to xeric savannas^{16,18}, hypothetically implying competition between grasses and mature trees for shallow soil water. The broadly positive relationship between tree cover and rainfall frequency may indicate that trees can exploit surface soil water better than grasses at this MAR range, leading to tree dominance and out-competition of shade-intolerant grasses. This is an interesting finding in our opinion, suggesting that, differently from dry savannas, tree access to deep water is not as relevant in mesic savannas, as also suggested by field observations of ref.¹⁸, although it is important to temper this finding with reference to the relatively lower explanatory power of rainfall frequency on vegetation cover at this range.

Whereas rainfall frequency in the wet season is included as a predictor in the best models in the low and intermediate ranges, in the higher MAR range increasing rainfall intensity appears to be negatively correlated with tree cover, aligned with earlier findings in relation to rainfall intensity and tree cover^{9,42}. Indeed, rainfall intensity is the only variable included in the best model for TGB tree cover in this range. As there is a negative correlation between rainfall frequency and intensity in this MAR range (Pearson's $r = -0.41$), this result is also in line with what has been observed at intermediate MAR (for the most part), and with recent findings by ref.³⁶, i.e. increases in daily rainfall frequency are associated with increases in tree cover. However, although rainfall intensity remains the best predictor for tree cover, its decrease with rainfall intensity is also partially due to the simultaneous increase of rainfall intensity with both MAR, SI and $\log_{10}(\text{AFI})$, as shown by the residual analysis. Hence the signal identified linking rainfall intensity with tree cover is partly noisy.

Overall, although our results support a role for intra-seasonal rainfall variability for trees and grasses in different MAR ranges, our understanding of the mechanisms that lead to vegetation responses is still necessarily limited and speculative. Soil hydrology is complex and an approach taking into account its dynamics explicitly would be needed to proceed further. To understand the benefits to plants of the temporal distribution of rainfall, soil water availability is key, and this depends on a series of factors that also feedback to the vegetation itself, forming a complex system. Although more rare events can be beneficial for vegetation at low precipitation and less beneficial at high precipitation²², the picture here is complicated by water competition between trees and grasses, which should be properly disentangled by including the changes in dynamics along a rainfall gradient, for example including the MAR-dependent relative rooting depth of tree and grasses¹⁸. Tree access to deep water during the dry season may generate long-term memory effects⁷³, and contribute to different phenology of trees and grasses⁷⁴, which can lead to a temporal niche-partitioning⁴⁸, a known mechanism of species coexistence (the so-called storage-effect)⁴⁴. Soil texture influences water availability, and it thus mediates the response of tree cover to intra-seasonal rainfall variability, with a role that can be almost as important as total yearly rainfall^{9,19}. Finally, we would like to acknowledge that the scale of the hydrological dynamics of tree-grass water competition is much finer than the scale of the data used in the present study (0.5°). Given this resolution, the intra-seasonal rainfall variables here considered displayed very small variations in their mean values. However, these variations are seemingly relevant for vegetation, with local relationship possibly scaling up and emerging at the coarser scale of this analysis.

TGBs are likely to show contrasting responses to anthropogenic climate change, which is expected to increase rainfall intensity across Africa³⁵, depending on the absolute values of mean annual rainfall. If this increase will be accompanied by a decrease of rainfall frequency, our results suggest that grasses will decrease in dry TGBs possibly favouring further woody encroachment, while woody cover will be limited in mesic and humid savannas. Our findings suggest that intra-seasonal rainfall variability is especially important for grasses and trees in mesic TGBs. For these areas in particular, our research serves to enhance the so-far-limited understanding of the factors determining the relative balance of these two vegetation life-forms.

Data Availability

The observational datasets used in this study are all freely available. The TRMM 3B42 dataset is available at <https://mirador.gsfc.nasa.gov/>. The ESA CCI-LC, v 1.6.1 dataset is available at <http://maps.elie.ucl.ac.be/CCI/viewer/download.php>. The MODIS datasets (MOD44B and MOD45A1) are available at <https://earthdata.nasa.gov>. Post-processed data are available upon request to the authors.

References

- Parr, C. L., Lehmann, C. E. R., Bond, W. J., Hoffmann, W. A. & Andersen, A. N. Tropical grassy biomes: Misunderstood, neglected, and under threat. *Trends Ecol. Evol.* **29**, 205–213 (2014).
- Scholes, R. J. & Archer, S. R. Tree-Grass Interactions in Savannas. *Annu. Rev. Ecol. Syst.* **28**, 517–544 (1997).
- Murphy, B. P., Andersen, A. N. & Parr, C. L. The underestimated biodiversity of tropical grassy biomes. *Philos. Trans. R. Soc. B Biol. Sci.* **371**, 20150319 (2016).
- Bond, W. J. Ancient grasslands at risk. *Science* **351**, 120–122 (2016).
- D'Onofrio, D., von Hardenberg, J. & Baudena, M. Not only trees: Grasses determine African tropical biome distributions via water limitation and fire. *Glob. Ecol. Biogeogr.* **27**, 714–725 (2018).
- Oliveras, I. & Malhi, Y. Many shades of green: the dynamic tropical forest–savannah transition zones. *Philos. Trans. R. Soc. B Biol. Sci.* **371**, 20150308 (2016).
- Lehmann, C. E. R., Archibald, S. A., Hoffmann, W. A. & Bond, W. J. Deciphering the distribution of the savanna biome. *New Phytol.* **191**, 197–209 (2011).
- Sankaran, M. *et al.* Determinants of woody cover in African savannas. *Nature* **438**, 846–849 (2005).
- Case, M. F. & Staver, A. C. Soil texture mediates tree responses to rainfall intensity in African savannas. *New Phytol.* **219**, 1363–1372 (2018).
- Dantas, V., de, L., Hirota, M., Oliveira, R. S. & Pausas, J. G. Disturbance maintains alternative biome states. *Ecol. Lett.* **19**, 12–19 (2016).

11. Staver, A. C., Archibald, S. & Levin, S. A. The global extent and determinants of savanna and forest as alternative biome states. *Science* **334**, 230–232 (2011).
12. Hirota, M., Holmgren, M., Van Nes, E. H. & Scheffer, M. Global Resilience of Tropical Forest and Savanna to Critical Transitions. *Science* **334**, 232–235 (2011).
13. Yin, Z., Dekker, S. C., van den Hurk, B. J. J. M. & Dijkstra, H. A. The climatic imprint of bimodal distributions in vegetation cover for western Africa. *Biogeosciences* **13**, 3343–3357 (2016).
14. Staver, C. A. & Levin, S. Integrating Theoretical Climate and Fire Effects on Savanna and Forest Systems. *Am. Nat.* **180**, 211–224 (2012).
15. Walker, B. H. & Noy-Meir, I. In *Tropical savannas* (eds Huntley, B. J. & Walker, B. H.) 556–590 (Springer-Verlag, 1982).
16. Ward, D., Wiegand, K. & Getzin, S. Walter's two-layer hypothesis revisited: Back to the roots! *Oecologia* **172**, 617–630 (2013).
17. Holdo, R. M. & Nippert, J. B. Transpiration dynamics support resource partitioning in African savanna trees and grasses. *Ecology* **96**, 1466–1472 (2015).
18. Holdo, R. M., Nippert, J. B. & Mack, M. C. Rooting depth varies differentially in trees and grasses as a function of mean annual rainfall in an African savanna. *Oecologia* **186**, 269–280 (2018).
19. Noy-Meir, I. Desert Ecosystems: Environment and Producers. *Annu. Rev. Ecol. Syst.* **4**, 25–51 (1973).
20. Medvigy, D., Wofsy, S. C., Munger, J. W. & Moorcroft, P. R. Responses of terrestrial ecosystems and carbon budgets to current and future environmental variability. *Proc. Natl. Acad. Sci.* **107**, 8275–8280 (2010).
21. Guan, K. *et al.* Simulated sensitivity of African terrestrial ecosystem photosynthesis to rainfall frequency, intensity, and rainy season length. *Environ. Res. Lett.* **13**, 025013 (2018).
22. Baudena, M., Boni, G., Ferraris, L., Von Hardenberg, J. & Provenzale, A. Vegetation response to rainfall intermittency in drylands: Results from a simple ecohydrological box model. *Adv. Water Resour.* **30**, 1320–1328 (2007).
23. Chesson, P. *et al.* Resource pulses, species interactions, and diversity maintenance in arid and semi-arid environments. *Oecologia* **141**, 236–253 (2004).
24. Rodriguez-Iturbe, I. & Porporato, A. *Ecohydrology of water-controlled ecosystems: soil moisture and plant dynamics*. (Cambridge University Press, 2004).
25. D'Onofrio, D., Baudena, M., D'Andrea, F., Rietkerk, M. & Provenzale, A. Tree-grass competition for soil water in arid and semiarid savannas: The role of rainfall intermittency. *Water Resour. Res.* **51**, 169–181 (2015).
26. Yuan, C. & Chesson, P. The relative importance of relative nonlinearity and the storage effect in the lottery model. *Theor. Popul. Biol.* **105**, 39–52 (2015).
27. Verwijmeren, M. Interspecific facilitation and critical transitions in arid ecosystems. (Utrecht University, 2016).
28. Medvigy, D. & Beaulieu, C. Trends in daily solar radiation and precipitation coefficients of variation since 1984. *J. Clim.* **25**, 1330–1339 (2012).
29. New, M. *et al.* Evidence of trends in daily climate extremes over southern and west Africa. *J. Geophys. Res. Atmos.* **111** (2006).
30. Mason, S. J., Waylen, P. R., Mimmack, G. M., Rajaratnam, B. & Harrison, J. M. Changes in extreme rainfall events in South Africa. *Clim. Change* **41**, 249–257 (1999).
31. Batisani, N. & Yarnal, B. Rainfall variability and trends in semi-arid Botswana: Implications for climate change adaptation policy. *Appl. Geogr.* **30**, 483–489 (2010).
32. Aguilar, E. *et al.* Changes in temperature and precipitation extremes in western central Africa, Guinea Conakry, and Zimbabwe, 1955–2006. *J. Geophys. Res. Atmos.* **114** (2009).
33. Nicholson, S. E. Climate and climatic variability of rainfall over eastern Africa. *Rev. Geophys.* **55**, 590–635 (2017).
34. Min, S. K., Zhang, X., Zwiers, F. W. & Hegerl, G. C. Human contribution to more-intense precipitation extremes. *Nature* **470**, 378–381 (2011).
35. Nikulin, G. *et al.* The effects of 1.5 and 2 degrees of global warming on Africa in the CORDEX ensemble. *Environ. Res. Lett.* **13**, 065003 (2018).
36. Xu, X., Medvigy, D., Trugman, A. T., Guan, K. & Rodriguez-iturbe, S. P. G. I. Tree cover shows strong sensitivity to precipitation variability across the global tropics. *Glob. Ecol. Biogeogr.* **27**, 450–460 (2018).
37. Guan, K. *et al.* Continental-scale impacts of intra-seasonal rainfall variability on simulated ecosystem responses in Africa. *Biogeosciences* **11**, 6939–6954 (2014).
38. Kulmatiski, A. & Beard, K. H. Woody plant encroachment facilitated by increased precipitation intensity. *Nat. Clim. Chang.* **3**, 833–837 (2013).
39. February, E. C. & Higgins, S. I. The distribution of tree and grass roots in savannas in relation to soil nitrogen and water. *South African J. Bot.* **76**, 517–523 (2010).
40. Baudena, M., D'Andrea, F. & Provenzale, A. An idealized model for tree–grass coexistence in savannas: the role of life stage structure and fire disturbances. *J. Ecol.* **98**, 74–80 (2010).
41. February, E. C., Higgins, S. I., Bond, W. J. & Swemmer, L. Influence of competition and rainfall manipulation on the growth responses of savanna trees and grasses. *Ecology* **94**, 1155–1164 (2013).
42. Good, S. P. & Caylor, K. K. Climatological determinants of woody cover in Africa. *Proc. Natl. Acad. Sci.* **108**, 4902–4907 (2011).
43. Xu, X., Medvigy, D. & Rodriguez-iturbe, I. Relation between rainfall intensity and savanna tree abundance explained by water use strategies. *Proc. Natl. Acad. Sci.* **112**, 12992–12996 (2015).
44. Chesson, P. Mechanisms of maintenance of species diversity. *Annu. Rev. Ecol. Syst.* **31**, 343–366 (2000).
45. Walsh, R. P. D. & Lawler, D. M. Rainfall seasonality: description, spatial patterns and change through time. *Weather* **36**, 201–208 (1981).
46. Rodriguez-Iturbe, I. Ecohydrology: A hydrologic perspective of climate-soil-vegetation dynamics. *Water Resour. Res.* **36**, 3–9 (2000).
47. Knapp, A. K. *et al.* Consequences of More Extreme Precipitation Regimes for Terrestrial Ecosystems. *Bioscience* **58**, 811–821 (2008).
48. Sankaran, M., Ratnam, J. & Hanan, N. P. Tree-grass coexistence in savannas revisited - Insights from an examination of assumptions and mechanisms invoked in existing models. *Ecology Letters* **7**, 480–490 (2004).
49. Roy, D. P., Boschetti, L., Justice, C. O. & Ju, J. The Collection 5 MODIS Burned Area Product - Global Evaluation by Comparison with the MODIS Active Fire Product. *Remote Sens. Environ.* **112**, 3690–3707 (2008).
50. Roy, D. P., Jin, Y., Lewis, P. E. & Justice, C. O. Prototyping a global algorithm for systematic fire-affected area mapping using MODIS time series data. *Remote Sens. Environ.* **97**, 137–162 (2005).
51. Roy, D., Lewis, P. & Justice, C. Burned area mapping using multi-temporal moderate spatial resolution data—a bi-directional reflectance model-based expectation approach. *Remote Sens. Environ.* **83**, 263–286 (2002).
52. Johnson, E. A. & Wagner, C. E. Van. The theory and use of two fire history models. *Can. J. For. Res.* **15**, 214–220 (1985).
53. Lehsten, V., Harmand, P., Palumbo, I. & Arneth, A. Modelling burned area in Africa. *Biogeosciences* **7**, 3199–3214 (2010).
54. Townshend, J. R. *et al.* Vegetation Continuous Fields MOD44B, 2000–2010 Percent Tree Cover, Percent Non-Tree Vegetation, Collection 5, Version 051, University of Maryland, College Park, Maryland. (Digital data accessed 08/12/2016 from, <https://earthdata.nasa.gov/>) (2011).
55. Bucini, G. & Hanan, N. P. A continental-scale analysis of tree cover in African savannas. *Glob. Ecol. Biogeogr.* **16**, 593–605 (2007).
56. Bowman, D. M. J. S. & Prior, L. D. Why do evergreen trees dominate the Australian seasonal tropics? *Aust. J. Bot.* **53**, 379–399 (2005).
57. Shorrocks, B. *The biology of African savannas*. 1–9 (Oxford: OUP Premium, 2007).

58. Gerard, F. *et al.* MODIS VCF should not be used to detect discontinuities in tree cover due to binning bias. A comment on Hanan *et al.* (2014) and Staver and Hansen (2015). *Glob. Ecol. Biogeogr.* **26**, 854–859 (2017).
59. McCullagh, P. & Nelder, J. A. *Generalized Linear Models, Second Edition.* (Taylor & Francis, 1989).
60. Dobson Annette J. *An introduction to generalized linear models/Annette J. Dobson.* (Chapman & Hall/CRC Boca Raton, 2002).
61. Schwarz, M. & Zimmermann, N. E. A new GLM-based method for mapping tree cover continuous fields using regional MODIS reflectance data. *Remote Sens. Environ.* **95**, 428–443 (2005).
62. Akaike, H. A new look at the statistical model identification. *IEEE Trans. Automat. Contr.* **19**, 716–723 (1974).
63. Guisan, A. & Zimmermann, N. E. Predictive habitat distribution models in ecology. *Ecol. Modell.* **135**, 147–186 (2000).
64. Fay, P. A., Carlisle, J. D., Knapp, A. K., Blair, J. M. & Collins, S. L. Productivity responses to altered rainfall patterns in a C 4-dominated grassland. *Oecologia* **137**, 245–251 (2003).
65. Hipondoka, M. H., Aranibar, J., Chirara, C., Lihavha, M. & Macko, S. Vertical distribution of grass and tree roots in arid ecosystems of Southern Africa: niche differentiation or competition? *J. Arid Environ.* **54**, 319–325 (2003).
66. Kulmatiski, A. & Beard, K. H. Root niche partitioning among grasses, saplings, and trees measured using a tracer technique. *Oecologia* **171**, 25–37 (2013).
67. Cabal, C. & Rubenstein, D. I. Above- and below-ground allocation and functional trait response to soil water inputs and drying rates of two common savanna grasses. *J. Arid Environ.* **157**, 1–12 (2018).
68. Mazzacavallo, M. G. & Kulmatiski, A. Modelling Water Uptake Provides a New Perspective on Grass and Tree Coexistence. **10**, e0144300 (2015).
69. Walter, H. K. *Vegetation of the earth in relation to climate and the eco-physiological conditions.* (London: English universities press, 1973).
70. Heisler-White, J. L., Blair, J. M., Kelly, E. F., Harmoney, K. & Knapp, A. K. Contingent productivity responses to more extreme rainfall regimes across a grassland biome. *Glob. Chang. Biol.* **15**, 2894–2904 (2009).
71. Swemmer, A. M., Knapp, A. K. & Snyman, H. A. Intra-seasonal precipitation patterns and above-ground productivity in three perennial grasslands. *J. Ecol.* **95**, 780–788 (2007).
72. Knapp, A. K. Rainfall Variability, Carbon Cycling, and Plant Species Diversity in a Mesic Grassland. *Science* **298**, 2202–2205 (2002).
73. Richard, Y. *et al.* Multi-month memory effects on early summer vegetative activity in semi-arid South Africa and their spatial heterogeneity. *Int. J. Remote Sens.* **33**, 6763–6782 (2012).
74. Guan, K. *et al.* Terrestrial hydrological controls on land surface phenology of African savannas and woodlands. *J. Geophys. Res. Biogeosciences* **119**, 1652–1669 (2014).

Acknowledgements

D. D'Onofrio and J. von Hardenberg acknowledge support from the European Union Horizon 2020 research and innovation programme under grant agreement No. 641816 (CRESCENDO) and from the Project of strategic Interest *NextData* of the Italian Ministry of Education, University and Research (MIUR) (<http://www.nextdataproject.it>).

Author Contributions

D.D. and L.S. share the first authorship. D.D. and M.B. conceived the original idea. D.D. and L.S. performed the data analysis, with contributions from J.H. and M.B. D.D. and L.S. wrote the first draft of the manuscript and all authors contributed substantially to the revisions.

Additional Information

Supplementary information accompanies this paper at <https://doi.org/10.1038/s41598-019-38933-9>.

Competing Interests: The authors declare no competing interests.

Publisher's note: Springer Nature remains neutral with regard to jurisdictional claims in published maps and institutional affiliations.



Open Access This article is licensed under a Creative Commons Attribution 4.0 International License, which permits use, sharing, adaptation, distribution and reproduction in any medium or format, as long as you give appropriate credit to the original author(s) and the source, provide a link to the Creative Commons license, and indicate if changes were made. The images or other third party material in this article are included in the article's Creative Commons license, unless indicated otherwise in a credit line to the material. If material is not included in the article's Creative Commons license and your intended use is not permitted by statutory regulation or exceeds the permitted use, you will need to obtain permission directly from the copyright holder. To view a copy of this license, visit <http://creativecommons.org/licenses/by/4.0/>.

© The Author(s) 2019